PAPER

Check for updates

High-performance low temperature curable copolyimides *via* multidimensional modulation in alkaline environment and electronic effects of monomers†

Xialei Lv,‡[a] Shan Huang,‡[ab] Zimeng He,[a] Jinhui Li, [iD] *[a] Siyao Qiu,[a] Tao Wang,[a] Yun Bai,[a] Yao Zhang,[a] Guoping Zhang [iD] *[a] and Rong Sun [iD] [a]

A new design strategy for the preparation of copolyimides (co-PIs) with low curable temperature (200 °C) for IC packages and liquid crystal displays is presented. Firstly, two novel pyrimidine-based diamines named MePMNH$_2$ and 2MePMNH$_2$ were designed and synthesized, the electron-donating ability and alkalinity of which were effectively adjusted by the states of the methyl group at the *meta-* or *ortho-*/*para-*position of the N atom in pyrimidine. The co-PI film of ODA and ODPA with 5 wt% 2MePMNH$_2$, which was cured at a low temperature of 200 °C, showed greatly improved properties with a Young's modulus of 4.1 GPa, elongation of 21.1%, a tensile strength of 163 MPa, and a 5% decomposition temperature ($T_{d,5\%}$) of 515 °C compared with the reference PI films (without 2MePMNH$_2$). Moreover, the intrinsic D_k and dielectric loss values of PI-Me$_{20\%}$-200 cured at 200 °C were reduced to 3.13 and 0.0089 at 10 GHz. The excellent dielectric performance of MePMNH$_2$ and good solubility were in agreement with its more twisted structures, which was verified by theoretical calculations. Increased alkalinity and electron-donating ability of diamines promoted the imidization process by lowering the energetic barrier and accelerating the cyclization reaction, as evidenced by the reduced curing temperature and improved comprehensive performances. Besides, the structural regulation of diamines also facilitated the cyclization reaction to some degree. This work not only provides efficient monomers based on a pyrimidine building block, but also sheds light on the inherent mechanism between structure and properties, and paves the way to designing highly promising PI films utilized in advanced packaging.

1. Introduction

Low temperature curable polyimides (PIs) are gaining increased attention because of their potential applications for advanced packaging and liquid crystal displays.[1,10] Traditional PIs are usually prepared by thermal curing at 300–400 °C to ensure complete imidization, thereby obtaining outstanding thermal stability, excellent mechanical properties, acceptable dielectric properties and so on.[2–4] As is known to all, PI materials are good candidates in passivation layers, photosensitive polyimides, electrical insulators, substrates for flexible printed circuit boards of OLED displays, *etc.*[5] Nonetheless, the high curing temperature would be harmful to adjacent components, or produce a mismatch between adjacent layers due to the stress difference. Accordingly, high-performance PI materials with low curing temperatures (≤200 °C) are of particular concern.[1,6,10]

Usually, there are three approaches to preparing low-temperature curing PIs,[7–10] (1) one step synthesis with a catalytic solvent; (2) adding curing agents; and (3) designing new monomers. One step synthesis applies to flexible diamines and dianhydrides, which draws support from autocatalysis of solvents, like phenols and carboxylic acids.[11] To a certain extent, the amide acid produced can also be used as a catalyst for the reaction itself. However, this method is subject to the limit of solubility and processing requirements, and high boiling point solvents are unfavorable for the environment and health. The second method is more universal *via* adding carboxylic acid, imidazole or tertiary amine catalysts as reported in the literature.[7,12–16] Hydroxycarboxylic acids showed a good catalytic effect, but the adding amount was large and they were then

[a] *Shenzhen International Innovation Institutes of Advanced Electronic Materials, Shenzhen Institutes of Advanced Technology, Chinese Academy of Sciences, Shenzhen 518055, China. E-mail: jh.li@siat.ac.cn, gp.zhang@siat.ac.cn*

[b] *Department of Nano Science and Technology Institute, University of Science and Technology of China, Suzhou, 215123, China*

† Electronic supplementary information (ESI) available. See DOI: https://doi.org/10.1039/d2ma00991a

‡ These authors contributed equally to this work.

difficult to completely remove.[14] The catalytic effect of nitrogen heterocyclic catalysts was related to alkalinity, the matching of the volatilization rate and imidization degree.[15] Nucleophilic catalysis of tertiary amines also promotes the amidation reaction of polyamides.[13] Nevertheless, the steric hindrance effect has a great influence on tertiary amine catalysts. Although curing agents could shorten the curing time, the removal of some catalysts was a tough problem to solve, and the additives that remained could be harmful to mechanical properties. In view of this, designing new monomers is the most promising way. There are several rules to design new monomers according to the imidization principle: (1) increase the activity of molecular chains; (2) reduce the interaction between chains; and (3) increase the nucleophilicity of diamines to attack carbonyl carbon. Leu *et al.* introduced flexible groups and large side groups in the monomers, increasing the molecular chain activity and the solubility, rendering a total imidization of PI after a 6 h reaction under 180 °C in *N*-methyl pyrrolidine (NMP).[17] Li *et al.* synthesized a diamine with a pyrazine unit and achieved a significant improvement in the imidization degree (ID) of PI films of 13.3% under 200 °C.[18] However, the rigid skeleton of diamine led to a lower ID. These reports enlightened the design and expansion of new monomers; yet, the design strategies of monomers are limited.[9,17–20]

In this work, we designed two new diamines with a pyrimidine group and different modifications of the methyl side group, named 4,4′-((5-methylpyrimidine-2,4-diyl)bis(oxy))dianiline (MePMNH$_2$) and 4,4′-((6-methylpyrimidine-2,4-diyl)bis(oxy))dianiline (2MePMNH$_2$). The alkaline autocatalytic effect and electron-donating ability of diamines were two important factors for the imidization process, of which the quantization and adjustment have not been studied before. The pyrimidine nitrogenous heterocycle has been proved to have an alkaline autocatalytic effect in our previous work; moreover, concurrently improving the electron-donating capacity of diamine could further increase the ability of amide nitrogen to attack carbonyl carbon. The substitution position of the methyl side group not only affects the electron-donating ability and alkalinity, but also has a different steric effect, which meticulously adjusted the copolyimide (co-PI) properties. Correspondingly, co-PIs realized an ID of 99.5% at a low curable temperature of 200 °C for 2MePMNH$_2$. When the methyl unit attached to the *meta*-position of the N atom in MePMNH$_2$, the highly twisted dihedral angle induced lower intrinsic D_k and dielectric loss values of PI-Me$_{20\%}$-200 (D_k = 3.13, and D_f = 0.0089 at 10 GHz), and good solubility. As for 2MePMNH$_2$, the stronger alkaline and electron-donating ability ensured the co-PI film a high imidization degree of 98.9% cured at 200 °C even doped with 5 wt% new monomers. Besides, PI-2Me$_{5\%}$-200 exhibited desired mechanical and thermal properties, a Young's modulus of 4.1 GPa, elongation of 21.1%, a tensile strength of 163 MPa and $T_{d,5\%}$ of 515 °C. Above all, the aim of this work is to provide an insight into the design of low-temperature curable polymers with high-performance, relevant to important advances in the development of materials in the microelectronics industry.

2. Experiment

2.1. Materials

N,N-Dimethylformamide (DMF) (99.8%), *N,N*-dimethylacetamide (DMAc) (99.8%) and tetrahydrofuran (THF) were provided from Energy Chemical Co., Ltd. 4,4-Oxydiphthalic anhydride (ODPA) (99.0%) and 4,4′-oxydianiline (ODA) (99.9%) were obtained from Tokyo Chemical Industry (TCI) Co., Ltd. ODA and ODPA were dried at 60 °C and 160 °C, respectively, in a vacuum oven for 10 h prior to use. The other raw materials for synthesis including 2,4-dichloro-5-methylpyrimidine, 2,4-dichloro-6-methylpyrimidineand, 85% hydrazine hydrate, 10% Pd/C, potassium carbonate and *p*-nitrophenol were all commercially available and used without any further purification.

2.2. Preparation of ODA/ODPA PI films

Firstly, 10.00 mmol (2.0024 g) ODA was added into 20 mL DMAc in a three-necked flask and mixed with a mechanical paddle under a nitrogen atmosphere at room temperature. Then, 10.00 mmol (3.1021 g) ODPA was evenly divided into two parts and added to the above solution in turn after the diamine was completely dissolved, and the solid content of the reaction solution was controlled at around 15%. Finally, the polyamide acid (PAA) solution was obtained after stirring for 12 h under nitrogen at room temperature and then spin-coated on the clean glass. After that, the PI films were got *via* different thermal curing processes, taking 200 °C and 350 °C as their final curing temperature, where we named them PI-200 and PI-350. The heating speed was 5 °C min^{-1} and stayed invariant at 100 °C for 1 h, 200 °C for 1 h, 300 °C for 1 h, and 350 °C for 1 h, or 100 °C for 1 h, and 200 °C for 3 h.

2.3. Preparation of (MePMNH$_2$/ODA)/ODPA co-PI films

The copolymerization of a pyrimidine-based diamine with ODA and ODPA was aimed to endow the PI films with low-temperature curable nature and satisfactory comprehensive performance. The PAAs were synthesized with various ratios of MePMNH$_2$ to ODA: 0.5/9.5, 1/9, 2/8 and 3/7, and the prepared films were named PI-Me$_x$–y, where x represents the proportion of MePMNH$_2$ to the total molar amount of diamine and y represented the final curing temperature. The thermal curing procedure of the co-PI films was the same as the preparation of ODA/ODPA PI films.

2.4. Preparation of (2MePMNH$_2$/ODA)/ODPA co-PI films

The PAAs were synthesized with various ratios of 2MePMNH$_2$ to ODA: 0.2/9.8, 0.5/9.5, 1/9 and 2/8, and the prepared films were also named PI-2Me$_x$–y, where x was the proportion of 2MePMNH$_2$ in the diamine monomers and y represented the final curing temperature, taking 200 °C and 350 °C as their final curing temperature.

2.5. Synthesis and characterization

The designed monomer of MePMNH$_2$ and 2MePMNH$_2$ was synthesized by the nucleophilic aromatic substitution reaction and reduction reaction as shown in Scheme S1 (ESI†). In particular, the reaction time was reduced to about 10 min after
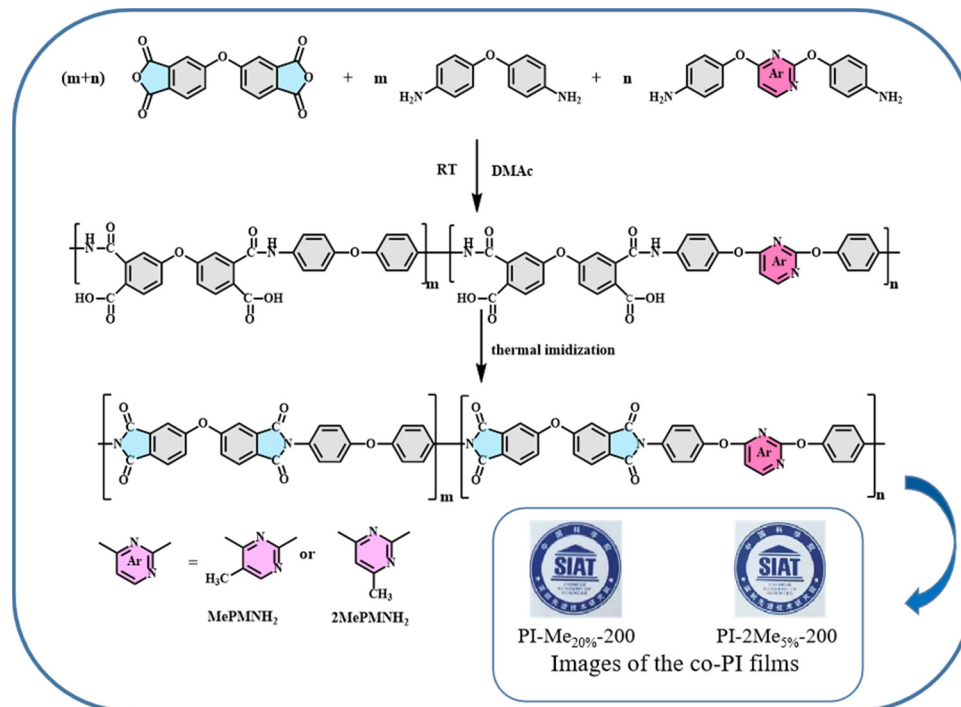
Fig. 1 Synthesis of the co-PI films and transparent photographs of PI-Me$_{20\%}$-200 and PI-2Me$_{5\%}$-200.

optimization of reduction reaction conditions for 2MePMNH$_2$. Additionally, the synthetic yields were all beyond 80%. Besides, all the intermediates and end products were confirmed by the nuclear magnetic resonance (NMR) and high resolution mass spectrometry (HRMS) as described in the ESI†(see Fig. S1–S3). In order to ensure the terpolymerization, the high performance liquid chromatography (HPLC) tests were also carried out for MePMNH$_2$ and 2MePMNH$_2$, while they both showed a high purity beyond 99% as seen in Fig. S4 (ESI†). The homopolymers and copolymers of PI films were synthesized with a two-step thermal imidization procedure as shown in Fig. 1. The detailed procedure was described in the experimental part. More encouragingly, the co-PI films cured at 200 °C exhibited high transparency even when the doping ratio achieved 20 wt% as seen in the inner pictures of Fig. 1, which demonstrated the potential of application in flexible displays.

3. Results and discussion

3.1. Infrared analysis and XRD patterns

The FTIR spectra of the PI films are shown in Fig. 2 and Fig. S5 (ESI†). The characteristic absorption bands at 1780 cm^{-1} and 1710 cm^{-1} (C=O asymmetric and symmetric stretching in the imide ring) and 1368 cm^{-1} for the stretching vibration of C–N in the imide ring were observed in all co-PI films cured at 200 °C. The characteristic absorption bands of the methyl group could be clearly seen in FTIR spectra of (2MePMNH$_2$/ODA)/ODPA co-PI films at about 1350 cm^{-1}, while it was not obvious in FTIR spectra of (MePMNH$_2$/ODA)/ODPA because it was overlapped with the characteristic peak of the imide ring. This variation was due to the different conjugation effects

between MePMNH$_2$ and 2MePMNH$_2$. Besides, the degree of imidization (ID) was evaluated by the integral area of peaks of stretching vibration of C–N and benzene ring as internal standard at 200 °C and 350 °C according to the reported method.[21–23] The IDs of co-PI films were substantially improved to 97.0–99.5% compared to that of the control sample PI-200 (with ODPA : ODA = 1 : 1) 93.5% when cured at 200 °C, showing a growing trend with the addition of MePMNH$_2$ and 2MePMNH$_2$. These results indicated that the introduction of pyrimidinyl diamine played a significant base catalyst in promoting imidization in low temperature (200 °C) process and the presence of electron-donating group methyl further enhanced the catalytic effect of the pyrimidine ring by accelerating the cyclization reaction.[24]

The XRD patterns of the co-PI films were also measured to see the arrangement of the molecular chain (as shown in Fig. S6, ESI†). The broad diffraction peak of co-PI films indicated their amorphous nature, and PI with ODPA often showed extremely broad diffraction peaks due to the flexible structure resulting in low crystallinity.[25,26] The solubility in polar aprotic organic solvents (NMP, DMF, DMAc, DMSO and THF) of the resulting PI films cured at 200 °C was also tested, and the results are shown in Table S2 (ESI†). In general, the PI films prepared by thermal curing is insoluble; yet, the solubility of the PI films cured at 200 °C in this work was comparable or even better than the reported ones.[27,28] It is interesting to note that PI-Me$_{20\%}$-200 had the best solubility among all samples, which might be ascribed to the larger distance between molecules. The good solubility of PI-Me$_{20\%}$-200 and PI-Me$_{30\%}$-200 made them good candidates in solution-processability and showed a good prospect for application in the microelectronics field.
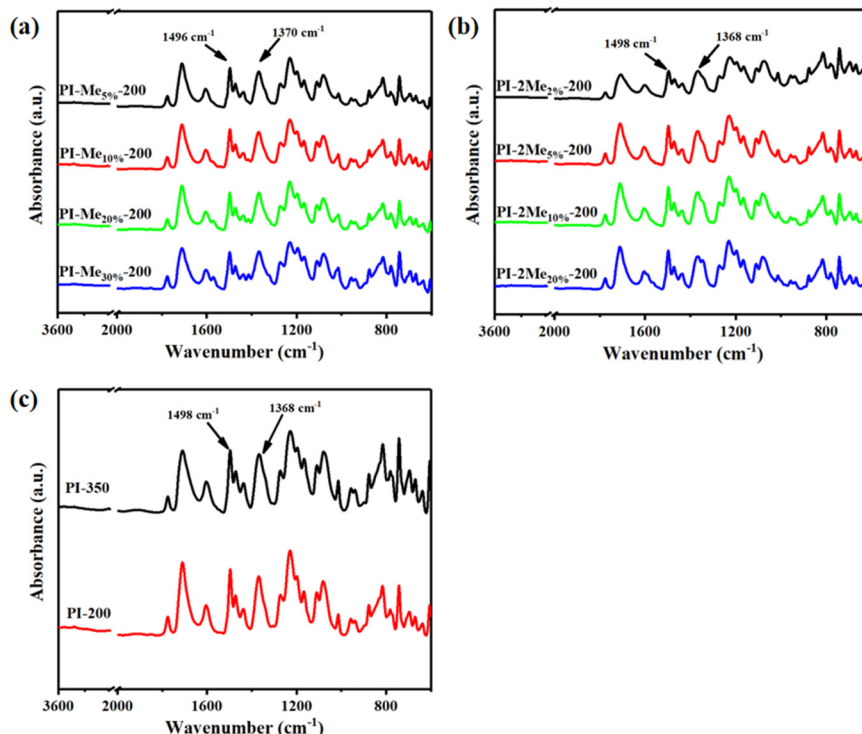
Fig. 2 FTIR spectra of (a) (MePMNH$_2$/ODA)/ODPA co-PI films cured at 200 °C, (b) (2MePMNH$_2$/ODA)/ODPA co-PI films cured at 200 °C and (c) ODA/ODPA PI films cured at 200 °C and 350 °C.

3.2. Thermal properties

The dimensional stability is important for PI films in the application of advanced packaging. Therefore, the coefficient of thermal expansion (CTE) values was tested by TMA, and the curves are illustrated in Fig. 3 and Fig. S7 (ESI†). The CTE of PI-200 was 57.09 ppm K^{-1}, and the CTE of PI-2Me$_{5\%}$-200 was 48.55 ppm K^{-1}, PI-Me$_{10\%}$-200 was 46.23 ppm K^{-1}, respectively. These results indicate that the addition of appropriate MePMNH$_2$ and 2MePMNH$_2$ could reduce the CTE of co-PI films when cured at 200 °C due to the effect of electrostatic interactions of polar groups.[29,30] Moreover, the CTEs of most low temperature curing co-PI films were lower than those of the corresponding co-PI films imidized at 350 °C. This might be ascribed to the more intense molecular chain movement at higher temperatures and resulted in crisp arrangement for co-PI films with lower doped concentrations of MePMNH$_2$ and 2MePMNH$_2$. In order to further verify the arrangement of molecules, we characterized the in-plane orientation of the PI films by linearly polarized IR spectroscopy and calculated the dichroic ratio (R). According to the reported literature,[31,32] R was evaluated by the absorbance area of IR at an angle of polarization 0° (IR beam parallels to X-axis direction, $A_{0°}$), 90° (IR beam perpendicular to X-axis direction, $A_{90°}$) and 180° (IR beam parallels to X-axis direction, $A_{180°}$), respectively. Considering the stretching vibration of C–N in the imide ring at about 1368 cm^{-1} was paralleled to the molecular chain, R of 1368 cm^{-1} was selected to depict in-plane molecular orientation. The absorbance at 1368 cm^{-1} of co-PI films decreased from 0° to 90° and increased to 180° as shown in Fig. S8(b) (ESI†). It is easy to find that the CTEs were significantly negatively correlated with the values of R under the influence of

curing temperature and blending ratios of MePMNH$_2$ and 2MePMNH$_2$. PI-2Me$_{5\%}$-200 had the highest R with a value of 2.30 among (2MePMNH$_2$/ODA)/ODPA co-PI films, while it showed the lowest CTE of 48.55 ppm K^{-1}. Similarly, PI-Me$_{10\%}$-200 exhibited a higher degree of orientation ($R = 2.17$) and a lower CTE among (MePMNH$_2$/ODA)/ODPA co-PI films. It is worth noting that dimensional stability was closely correlated with the degree of orientation, which is also influenced by molecular structures, movements, and intermolecular interactions.

The TGA curves of the co-PI films were also measured to investigate the thermal stability (see Fig. 3c, d and Fig. S9, ESI†). The thermal degradation temperatures of 5% and 10% ($T_{d,5\%}$ and $T_{d,10\%}$) and residual weight ratio at 800 °C ($R_{800 °C}$) in nitrogen atmosphere of the PI films are listed in Table 2 and Table S3 (ESI†). It suggests that when the doped proportion of pyrimidine diamine was lower than 5 wt%, the $T_{d,5\%}$ values for PI-Me$_{5\%}$-200, PI-2Me$_{2\%}$-200 and PI-2Me$_{5\%}$-200 films were higher than that of PI-200 (511 °C), and even comparable to PI-350 (516 °C). However, when the blending proportion was larger than 5 wt%, the $T_{d,5\%}$ values for co-PI films showed a gradual decrease trend with the increase of MePMNH$_2$ or 2MePMNH$_2$. This can be explained by the significantly improved ID playing a leading role in enhancing the thermal stability at lower doped concentrations, yet the decrease in $T_{d,5\%}$ values might be attributed to the decrease of benzene ring density at higher doped concentrations. The glass transfer temperature (T_g) of PI films was given by TMA. As shown in Table 2 and Table S3 (ESI†), the T_g value of co-PI films decreased with the increase of the addition of nitrogen doped
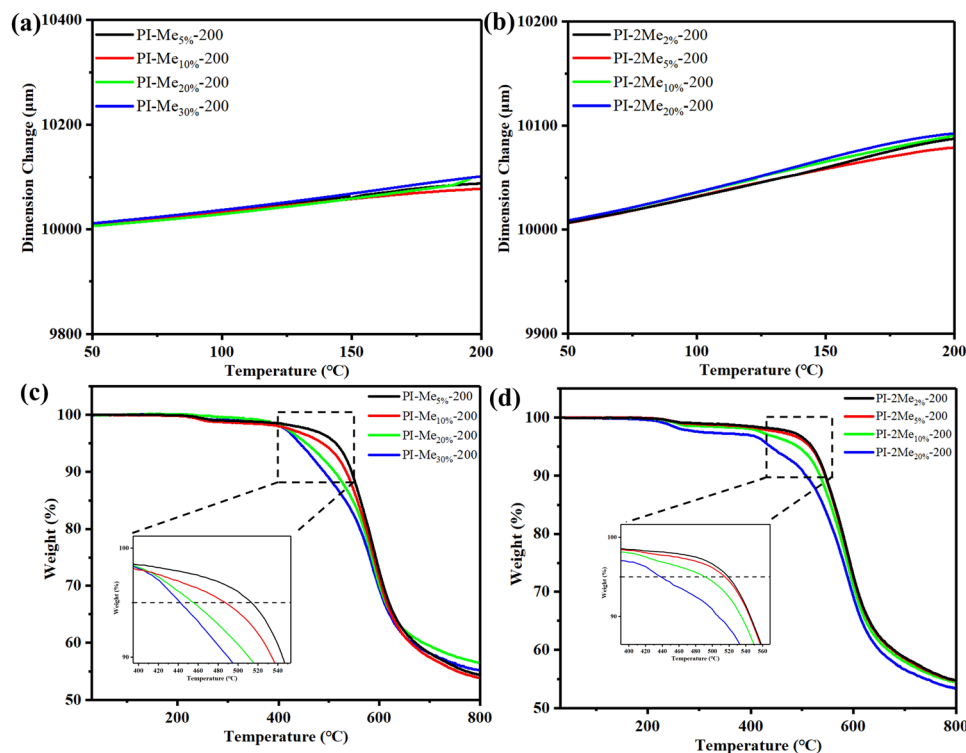
Fig. 3 TMA curves of (a) (MePMNH$_2$/ODA)/ODPA co-PI films and (b) (2MePMNH$_2$/ODA)/ODPA co-PI films; TGA curves of (c) (MePMNH$_2$/ODA)/ODPA co-PI films and (d) (2MePMNH$_2$/ODA)/ODPA co-PI films.

monomers when the curing temperature was 200 °C, ranging from 227 to 251 °C. This downward trend of T_g was attributed to the molecular chain of PI becoming increasingly mobile with the introduction of a side group.[26,30,33,34]

3.3. Mechanical properties

The marked rise in mechanical properties of the co-PI films cured at 200 °C is worth being concerned. The mechanical performances including tensile strength (σ), elongation at break (ε_b) and Young's modulus (E) were measured by DMA and shown in Fig. 4 and Fig. S10 (ESI†). As tabulated in Table 2, Young's modulus of most co-PI films was higher than PI-200, contributing to the higher ID. In particular, PI-2Me$_{5\%}$-200 had the best overall mechanical properties, with a tensile strength of 163 MPa, elongation of 21%, and Young's modulus of 4.1 GPa, which could be comparable or superior to most reported low-temperature PI films (as summarized in Table S5, ESI†). Moreover, this mechanical performance fully surpassed that of the PI-350. The reason for the excellent mechanical properties can be derived from the largest dichroic ratio ($R = 2.30$) calculated from the polarized attenuated total reflection/Fourier transform infrared spectroscopy, demonstrating a more regular molecular arrangement. Additionally, in the copolymerization system of MePMNH$_2$, PI-Me$_{20\%}$-200 exhibited better mechanical properties among them, slightly inferior to PI-2Me$_{5\%}$-200 due to the larger distance between molecular chains and less molecular arrangement regularity ($R = 2.16$).[35,36] PI-Me$_{30\%}$-200 showed unsatisfactory mechanical properties due to

the effect of the side groups and disordered molecular chains.[26,30,33,34]

3.4. Theoretical calculations

When developing a new monomer, it is instructive to quantitatively compare the alkalinity and chemical activity of diamine.[24,37,38] In this part, we tried to utilize theoretical calculations to investigate the pK_a values in DMAc solvent and the electron-donating ability of MePMNH$_2$ and 2MePMNH$_2$. Firstly, the distribution of electron cloud on the pyrimidine ring was increased by the introduction of electron-donating methyl, which facilitated the diamine to attack amidoacid fragments. And the pK_a values were attained by the polarizable continuum model (PCM), where protons bind with 7 DMAc molecules.[39,40] The calculated pK_a values were 17.65 for 2MePMNH$_2$, 17.05 for MePMNH$_2$, and 13.81 for ODA. This means that the alkalinity of 2MePMNH$_2$ was superior to MePMNH$_2$ and ODA. Secondly, the stronger electron-donating ability of diamine is profit for attacking carbonyl carbon in the preparation of aromatic polyamides. Furthermore, MePMNH$_2$ and 2MePMNH$_2$ had shallower HOMO (-5.32 eV and -5.30 eV) than similar pyrimidine based diamine PMNH$_2$ (-5.45 eV) in our previous work without a methyl substituent, which demonstrated that the introduction of methyl group indeed increased the electron-donating ability of diamine monomers.[41] In order to verify the accuracy, the cyclic voltammetry curves of three diamines were tested with a three-electrode system as seen in Fig. S11 (ESI†). The HOMO values evaluated from the onset of oxidation peaks were -5.10,
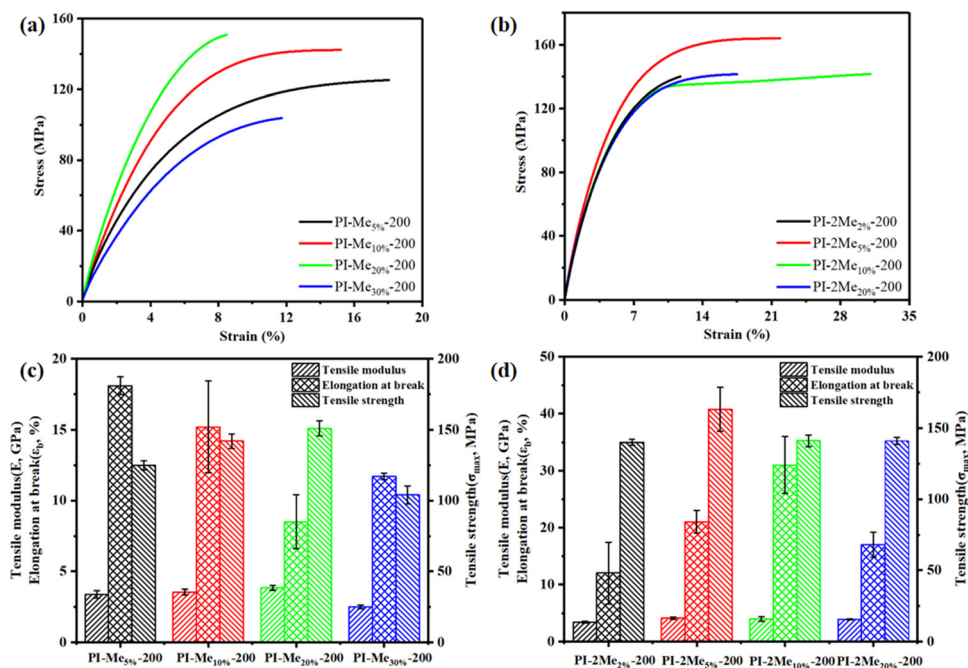
Fig. 4 Typical stress-strain curves of (a) (MePMNH$_2$/ODA)/ODPA co-PI films and (b) (2MePMNH$_2$/ODA)/ODPA co-PI films. Detailed data of mechanical properties of (c) (MePMNH$_2$/ODA)/ODPA co-PI films and (d) (2MePMNH$_2$/ODA)/ODPA co-PI films.
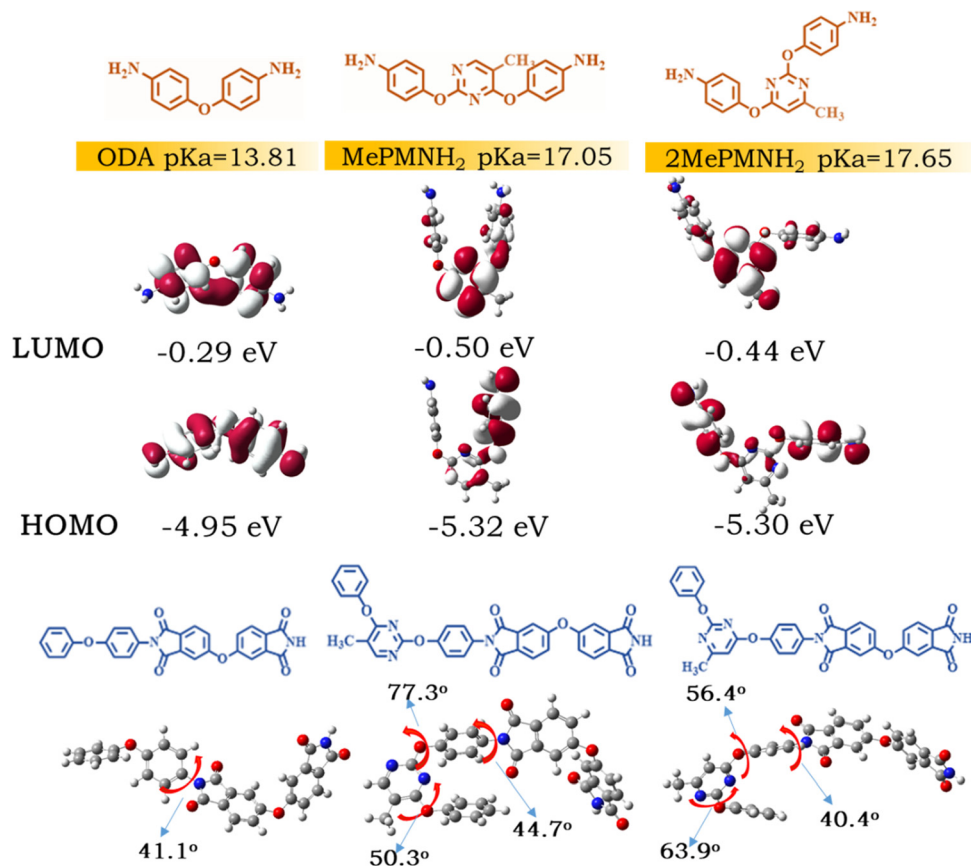

Fig. 5 The calculated pK_a values, HOMO (highest occupied molecular orbital)/LUMO (lowest unoccupied molecular orbital) distributions and energy levels of three diamines, and 3D structure of the mode compounds of ODPA and three diamines.

Table 1 Detailed data of ID, CTE and dichroic ratio of the resulting PI films cured at 200 °C

Sample name	ID (%)	CTE (ppm K^{-1})	Dichroic ratio	Diamine ratio (n)
PI-200	93.5	57.09	2.11	ODA
PI-Me$_{5\%}$-200	97.7	53.05	2.08	ODA : MePMNH$_2$ = 0.5 : 9.5
PI-Me$_{10\%}$-200	98.8	46.23	2.17	ODA : MePMNH$_2$ = 1.0 : 9.0
PI-Me$_{20\%}$-200	99.4	58.17	2.16	ODA : MePMNH$_2$ = 2.0 : 8.0
PI-Me$_{30\%}$-200	99.3	60.01	2.06	ODA : MePMNH$_2$ = 3.0 : 7.0
PI-2Me$_{2\%}$-200	97.0	50.25	2.12	ODA : 2MePMNH$_2$ = 0.2 : 9.8
PI-2Me$_{5\%}$-200	98.9	48.55	2.30	ODA : 2MePMNH$_2$ = 0.5 : 9.5
PI-2Me$_{10\%}$-200	99.1	55.50	2.07	ODA : 2MePMNH$_2$ = 1.0 : 9.0
PI-2Me$_{20\%}$-200	99.5	55.91	2.03	ODA : 2MePMNH$_2$ = 2.0 : 8.0

−5.28, and −5.26 eV for ODA, MePMNH$_2$ and 2MePMNH$_2$, respectively. The experimental results were consistent with the calculation tendency. Because of this, PI-2Me$_{5\%}$-200 achieving excellent comprehensive properties with a low doped concentration of 5 wt% can be explained. The methyl group introduced at the *ortho-/para*-position of the N atom in pyrimidine of 2MePMNH$_2$ could accelerate the cyclization reaction and reduce the energetic barrier of imidation more effectively than that of MePMNH$_2$.

Apart from this, the structural optimization was carried out by DFT[42] employing model compounds of ODA-ODPA, MePMNH$_2$-ODPA and 2MePMNH$_2$-ODPA, and the 3D molecular structures are depicted in Fig. 5. It can be observed that the torsion angle of MePMNH$_2$-ODPA between the pyrimidine ring and adjacent benzene ring was 77.3°, while the largest dihedral angle of ODA-ODPA was 41.1°. The steric hindrance of *ortho*-substituted methyl groups of MePMNH$_2$ caused a greater torsion angle, which induced a more transparent property. The transmittance of the resulting PI films was measured using a UV-vis spectrophotometer with a wavelength ranging from 300 to 800 nm as shown in Fig. S12 (ESI†) and Table 1. All 200 °C cured PI films showed excellent optical transparency with transmittance at 450 nm above 89%. The optical transparency of the films was also evaluated and the haze value of the films is summarized in Table 1. These results showed that MePMNH$_2$ based co-PI films cured at 200 °C had excellent optical transparency than the 2MePMNH$_2$ series, which could be ascribed to the more twisted structure. In this regard, the molecular dynamics simulation of these co-PI films showed a good consensus of experimental results.

3.5. Electrical properties

The dielectric constant (D_k) and dielectric loss (D_f) at high frequency are important parameters for 5G communication technology, attracting increased attention.[43] The dielectric properties of these PI films at 10 GHz are tested and listed in Table S4 (ESI†). These results indicate that the dielectric constant of the PI films was particularly associated with ID and polarizability. It is widely believed that PI films cured at 350 °C have better electrical properties than those cured at 200 °C because low temperature curing may result in more residual polar groups such as carboxyl groups in chains.[7,9,14] However, the rules were not completely applicable to this system due to the larger free volume derived from the methyl side group and highly twisted structures.[44–46] The D_k values decreased first and then increased by increasing 2MePMNH$_2$ or MePMNH$_2$ monomers, attributing to the increase in free volume and IDs at lower doped concentration and the effect of polar group pyrimidine at higher blending ratio beyond 10 wt%. Meanwhile, the D_k value of (MePMNH$_2$/ODA)/ODPA co-PI films were lower than (2MePMNH$_2$/ODA)/ODPA co-PI films with the same copolymerization ratio, indicating that methyl at the *ortho* position of nitrogen atom produced larger free volumes than those of 2MePMNH$_2$, which was in line with the calculation results. Based on this, PI-Me$_{20\%}$-200 exhibited a low D_k of 3.13 and a low D_f of 0.89%, which was among the best dielectric properties as shown in Table S5 (ESI†), even surpassed the dielectric properties of commercial kapton film (D_k = 3.41 and D_f = 1.57%). The contact angles of all PI films cured at 200 °C are listed in Table 2. The contact angle of PI-Me$_{10\%}$-200 and PI-2Me$_{5\%}$-200 was higher among their respective copolymerization systems. This result indicated that molecular arrangement might also act as a deciding factor instead of ID and polar units with a lower doped concentration of MePMNH$_2$/2MePMNH$_2$, which resulted in a first increase and then a decrease trend.

4. Conclusions

The key criteria for developing a low temperature curable PI system with excellent properties were laid out with regard to the

Table 2 Mechanical and thermal properties of the resulting PI films cured at 200 °C

Sample	Thermal properties				Mechanical properties			Other properties		
	TGA			TMA	DMA					
	$T_{d,5\%}$	$T_{d,10\%}$	$R_{800\ °C}$	T_g	σ_{max}	ε_b	E	Haze	Transmittance at 450 nm	Contact angle
	(°C)	(°C)	(%)	(°C)	(MPa)	(%)	(GPa)	(%)	(%)	(°)
PI-200	511	543	54.84	252	143	17.7	3.18	1.29	93.9	76.3
PI-Me$_{5\%}$-200	518	546	54.33	248	125	18.1	3.38	0.33	89.3	77.1
PI-Me$_{10\%}$-200	487	534	53.90	239	142	15.2	3.55	0.42	91.8	78.1
PI-Me$_{20\%}$-200	455	511	56.46	230	151	8.2	3.83	0.14	93.2	74.5
PI-Me$_{30\%}$-200	442	490	55.10	227	104	11.7	2.51	0.27	89.4	74.5
PI-2Me$_{2\%}$-200	519	546	54.72	251	140	11.7	3.40	0.47	94.1	78.1
PI-2Me$_{5\%}$-200	515	545	54.63	246	163	21.1	4.13	0.17	92.3	78.4
PI-2Me$_{10\%}$-200	491	535	54.41	240	141	31.0	4.02	0.20	92.3	77.6
PI-2Me$_{20\%}$-200	439	507	53.38	227	141	17.0	3.89	0.30	90.1	77.1

fundamental characteristics and theoretical calculations. The co-PI films prepared under 200 °C were colorless and showed high transparency owing to the twisted structure deriving from the methyl side group of MePMNH$_2$/2MePMNH$_2$. The co-PI film of ODA and ODPA with 5 wt% 2MePMNH$_2$ showed satisfactory mechanical properties (E = 4.1 GPa, ε_b = 21.1%, σ = 163 MPa) and favorable thermal properties ($T_{d,5\%}$ = 515 °C and T_g = 246 °C), much better than the reference PI films without 2MePMNH$_2$ cured at 200 °C. The outstanding mechanical performance was consistent with the results of molecular arrangement. MePMNH$_2$ with a methyl unit attached to the *meta*-position of a nitrogen atom produced excellent dielectric performance, good solubility and better transparency due to the larger free volume. The results demonstrated that the regulation of the methyl position had a profound influence on the structure, thermal, mechanical, dielectric and solubility properties of polyimides. This work also provided enlightenment for low doping and high performance low temperature curable diamine monomers and paved a new way to design candidate PI films utilized in advanced packaging.

Conflicts of interest

There are no conflicts to declare.

Acknowledgements

References

1 R. J. Iredale, C. Ward and I. Hamerton, *Prog. Polym. Sci.*, 2017, **69**, 1–21.

2 I. Gouzman, E. Grossman, R. Verker, N. Atar, A. Bolker and N. Eliaz, *Adv. Mater.*, 2019, **31**, 1807738.

3 M. Kaltenbrunner, T. Sekitani, J. Reeder, T. Yokota, K. Kuribara, T. Tokuhara, M. Drack, R. Schwodiauer, I. Graz and S. Bauer-Gogonea, *Nature*, 2013, **499**, 458–463.

4 D.-J. Liaw, K.-L. Wang, Y.-C. Huang, K.-R. Lee, J.-Y. Lai and C.-S. Ha, *Prog. Polym. Sci.*, 2012, **37**, 907–974.

5 B. Chen, X. Li, X. Li, Y. Jia, J. Yang and C. Li, *Polym. Compos.*, 2018, **39**, 1626–1634.

6 J. Kusunoki and T. Hirano, *J. Photopolym. Sci. Technol.*, 2005, **18**, 321–325.

7 C. Huang, J. Li, D. Sun, R. Xuan, Y. Sui, T. Li, L. Shang, G. Zhang, R. Sun and C. P. Wong, *J. Mater. Chem. C*, 2020, **8**, 14886–14894.

8 K.-S. Jang, D. Wee, Y. H. Kim, J. Kim, T. Ahn, J.-W. Ka and M. H. Yi, *Langmuir*, 2013, **29**, 7143–7150.

9 Y. Sui, J. Li, T. Wang, D. Sun, C. Huang, F. Zhang, L. Shan, F. Niu, G. Zhang and R. Sun, *Polymer*, 2021, **218**, 123514.

10 T. Sasaki, *J. Photopolym. Sci. Technol.*, 2016, **29**, 379–382.

11 A. A. Kuznetsov, *High Perform. Polym.*, 2000, **12**, 445–460.

12 M. Kotera, B. Samyul, K. Araie, Y. Sugioka, T. Nishino, S. Maji, M. Noda, K. Senoo, T. Koganezawa and I. Hirosawa, *Polymer*, 2013, **54**, 2435–2439.

13 Y. Ding, B. Bikson and J. K. Nelson, *Macromolecules*, 2002, **35**, 905–911.

14 M. Oba, *J. Polym. Sci., Part A: Polym. Chem.*, 1996, **34**, 651–658.

15 A. Nelson, G. Guerra, D. J. Williams, F. E. Karasz and W. J. Macknight, *J. Appl. Polym. Sci.*, 1988, **36**, 243–248.

16 Y. Xu, A. Zhao, X. Wang, H. Xue and F. Liu, *J. Wuhan Univ. Technol., Mater. Sci. Ed.*, 2016, **31**, 1137–1143.

17 T.-S. Leu and C.-S. Wang, *J. Polym. Sci., Part A: Polym. Chem.*, 2001, **39**, 4139–4151.

18 C. Li, Y. Wang, Y. Yin, Y. Li, J. Li, D. Sun, J. Lu, G. Zhang and R. Sun, *Polymer*, 2021, **228**, 123963.

19 X. Li, P. Zhang, J. Dong, F. Gan, X. Zhao and Q. Zhang, *Composites, Part B*, 2019, **177**, 107401.

20 Y. Zhuang, J. G. Seong and Y. M. Lee, *Prog. Polym. Sci.*, 2019, **92**, 35–88.

21 C. A. Pryde, *J. Polym. Sci., Part A: Polym. Chem.*, 1993, **31**, 1045–1052.

22 Y. Zhai, Q. Yang, R. Zhu and Y. Gu, *J. Mater. Sci.*, 2008, **43**, 338–344.

23 X. Jin and D. Zhu, *Eur. Polym. J.*, 2008, **44**, 3571–3577.

24 V. M. Svetlichnyi, N. G. Antonov, B. V. Chernitsa, V. M. Denisov, A. I. Koltsov, V. V. Kudryavtsev and M. M. Koton, *Vysokomol. Soedin., Ser. A*, 1986, **28**, 2412–2418.

25 B. Zhang, Y. Wu, Y. Lu, T. Wang, X. Jian and J. Qiu, *J. Membr. Sci.*, 2015, **474**, 14–121.

26 X. Zhang, B. Zhang, Y. Wu, D. Wang and T. Wang, *J. Appl. Polym. Sci.*, 2017, **134**, 44889.

27 Z. Li, K. Kou, J. Zhang, Y. Zhang, Y. Wang and C. Pan, *J. Mater. Sci.: Mater. Electron.*, 2017, **28**, 6079–6087.

28 J. Liu, J. Li, T. Wang, D. Huang, Z. Li, A. Zhong, W. Liu, Y. Sui, Q. Liu, F. Niu, G. Zhang and R. Sun, *Polymer*, 2022, **244**, 124660.

29 V. M. Nazarychev, S. V. Larin, A. V. Yakimansky, N. V. Lukasheva, A. A. Gurtovenko, I. V. Gofman, V. E. Yudin, V. M. Svetlichnyi, J. M. Kenny and S. V. Lyulin, *J. Polym. Sci., Part B: Polym. Phys.*, 2015, **53**, 912–923.

30 V. M. Nazarychev, A. V. Lyulin, S. V. Larin, I. V. Gofman, J. M. Kenny and S. V. Lyulin, *Macromolecules*, 2016, **49**, 6700–6710.

31 Y. Tian, L. Luo, Q. Yang, L. Zhang, M. Wang, D. Wu, X. Wang and X. Liu, *Polymer*, 2020, **188**, 122100.

32 S. I. Matsuda and S. J. Ando, *J. Polym. Sci.*, 2003, **41**, 418–428.

33 I. A. Ronova and M. Bruma, *Struct. Chem.*, 2010, **21**, 1013–1020.

34 X. Ma, F. Zheng, C. van Sittert and Q. Lu, *J. Phys. Chem. B*, 2019, **123**, 8569–8579.

35 Y. Feng, L. B. Luo, J. Huang, K. Li, B. Li, H. Wang and X. Liu, *J. Appl. Polym. Sci.*, 2016, **133**, 43677.

36 T. Zhang, Y. Huang, Y. Sun, P. Tang and C. Hu, *Polym. Adv. Technol.*, 2022, **33**, 2123–2136.

37 V. N. Artem'eva, V. V. Kudryavtsev, E. M. Nekrasova and V. P. Sklizkova, *Russ. Chem. Bull.*, 1994, **43**(3 387–390.

38 M. M. Koton, V. N. Artemeva, V. V. Kudryavtsev, Z. D. Chernova, N. V. Kukarkina, L. A. Ovsyannikova, G. D. Rudkovskaya, T. I. Zhukova and Y. P. Kuznetsov, *Vysokomol. Soedin., Ser. A*, 1983, **25**, 726–731.

39 F. Weigend and R. Ahlrichs, *Phys. Chem. Chem. Phys.*, 2005, **7**, 3297–3305.

40 C. T. Lee and W. T. Yang, *Phys. Rev. B: Condens. Matter Mater. Phys.*, 1988, **37**, 785–789.

41 X. Lv, S. Qiu, S. Huang, K. Wang and J. Li, *Polymer*, 2022, **261**, 125418.

42 C. Pu, D. Lin, H. Xu, F. Liu, H. Gao, G. Tian, S. Qi and D. Wu, *Polymer*, 2022, **255**, 125119.

43 K. Seo, K.-H. Nam, S. Lee and H. Han, *Mater. Lett.*, 2020, **263**, 127204.

44 S. H. Han, Y. N. Li, F. Y. Hao, H. Zhou, S. L. Qi, G. F. Tian and D. Z. Wu, *Eur. Polym. J.*, 2021, **143**, 110206.

45 Y. Luo, K. Jin, C. He, J. Wang, J. Sun, F. He, J. Zhou, Y. Wang and Q. Fang, *Macromolecules*, 2016, **49**, 7314–7321.

46 C. Qian, Z.-G. Fan, W.-W. Zheng, R.-X. Bei, T.-W. Zhu, S.-W. Liu, Z.-G. Chi, M. P. Aldred, X.-D. Chen, Y. Zhang and J.-R. Xu, *Chin. J. Polym. Sci.*, 2019, **38**, 213–219.